LABORATORY EXPERIMENTS ABOUT BED PATTERNS IN THE SHOALING REGION UNDER REGULAR WAVES AND REFLECTING CONDITIONS

Cobos M.[1], Clavero M., Baquerizo A., Longo, S.[2], Losada M.A.

This research is an experimental study of ripple dynamic for regular waves propagating on horizontal and sloping beds in mid- and high-reflective conditions. Small-scale laboratory experiments were carried out on shoaling region (with non breaking waves) and sediment transport in bedload regime. Our experiments showed the key role that plays the reflection in ripple development. The spatial modulation of the free surface elevation due to reflection created sandbars. Ripples grew up in the region where sandbars were appearing. These patterns were gradually reproduced from breakwater to offshore. The incidence of sandbar created a bi-modal structure of ripple geometry. The larger ripples appeared in the crest of sandbars whereas smaller ripples were found in the troughs. Furthermore, it was found that the evolution of ripples at these two locations can be explained by means of different growth mechanisms. Finally, at equilibrium stages, ripple height converges reaching the same height along the sandbar while ripple length and steepness remains almost constant.

Keywords: ripples; sandbars; reflection; sloping beaches

INTRODUCTION

Sand beaches are usually characterized by sand of different sizes and types. These grains are continuously evolving due to the shear forces that surface waves or currents generate at the near bed level. Despite the roughly uneven actions that take place, sediments self-organize in bedforms. These sediment structures have different spatio-temporal scales and are frequently related to the parameters that define the water motion. The knowledge of these natural structures is fundamental for the computation of wave energy dissipation, sediment transport rates or the explanation of deposition and erosion areas.

There is a large body of classical literature on analytical and empirical models, laboratory experiments and field studies that focus on the evolution and geometry of bedforms under stationary conditions [Manohar (1955), Inman (1957), Mogridge and Kamphuis (1972), Dingler (1974), Nielsen (1981), Allen (1982)]. Nielsen (1992) analyzed geometrical data of the ripples from lab experiments and field surveys to propose empirical approaches to describe ripples geometry under several flow conditions. They focused their analysis at the spatial domain, by capturing the length and height of a bedforms group from the bottom profile.

Doucette and O'Donoghue (2006) performed large-scale experiments to analyze the influence of wave randomness on the temporal evolution of ripples. The experimental results show that equilibrium ripple geometry is independent of initial bed morphology while the time to reach equilibrium is largely dependent of the initial bed and the equilibrium ripple size. Smith and Sleath (2005) analyzed the response time of the ripple-covered bed to a change in the flux conditions. Their results show that (i) the new profile keeps the wavelength when it arises from a previous perturbation of the same wavelength of the final profile; (ii) the ripple length gradually adjusts to the final ripple length when the initial perturbation has not the same wavelength. Other studies analyzed ripple growth and migration velocities under several conditions. Faraci and Foti (2002) described the ripple evolution under progressive regular and random waves for a flat bed.

More recent studies analyze the response time of the ripple-covered bed to a change in the flux conditions [Davis et al. (2004) or Traykovski (2007) as reference]. They described transition stages and relict shapes of ripples in the spectral domain.

However, near natural or artificial reflectors like cliffs, steep beaches or dikes, where waves reflect without breaking, the bedforms develop strongly related to the reflection process [see Benedicto et al. (2004), Sánchez-Badorrey et al. (2008), Baquerizo et al. (1997), Baquerizo et al. (2002), Baquerizo et al. (2005) and Ávila et al. (2008)]. Amongst the numerous questions, there are two questions still awaiting an answer: (i) what is the bedform evolution under partially reflective conditions, and (ii) how the bed slope affects the bed patterns evolution. A large set of experiments about ripple dynamics in the presence of a high- and low-reflective element was carried out by Landry (2011). He depicted some key elements governing the generation and their dynamic. A study about ripple and sandbar dynamics under mid-reflecting conditions,

[1]Instituto Universitario de Investigación del Sistema Tierra, Universidad de Granada, Avda. del Mediterráneo s/n, 18006 Granada, Spain

[2]Dipartimento di Ingegneria e Architettura (DIA), Università di Parma, Parco Area delle Scienze, 181/A, 43124 Parma, Italy

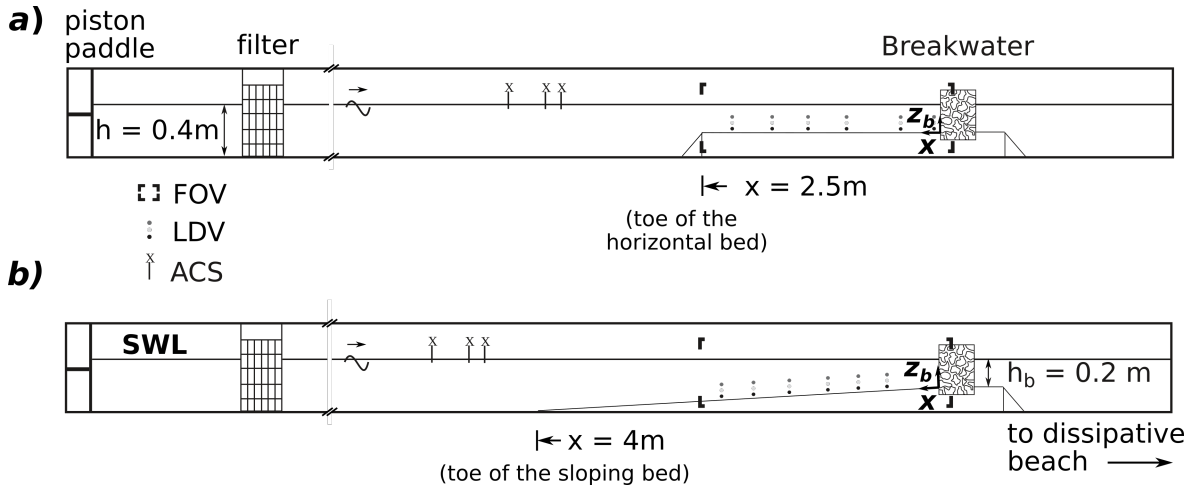

Figure 1: Layout of the flume. *a*) Tests with horizontal beds; *b*) tests with sloping beds. Field Of View (FOV) of the camera; LDV indicates the location of velocity records, ACS stands for the measurements of free surface elevation. A wooden table was placed in front of the porous breakwater in tests with high-reflecting conditions.

where waves do not break when propagated for a flat bed and with the sediment transport governed by bedload was recently presented by Cobos et al. (2016). The research study experimentally analyzed the bed pattern characteristic lengths and heights, growth rate and time to reach equilibrium in terms of the beach slope and the reflective character of the structure. Their experimental results showed that the concurrence of ripples and sand-bars under partially horizontal bottom reflected waves has a spatially modulating effect on ripple characteristics (i.e. growth, shape and migration celerity). This study uses the spectral analysis to depict and highlight some experimental evidences of ripple and sandbar dynamics under mid- and full-reflective conditions. The paper is organized as follows. Section 2 depicts the experimental setup and procedure. Section 3 describes the bottom morphology as well as the growth rate of the ripples. Section 4 discusses the key elements in the ripple growth and concludes this research.

EXPERIMENTAL SETUP AND PROCEDURE

Test facility

The laboratory experiments were carried out in the combined wave-current flume of the Andalusian Institute of Earth System Research (IISTA, University of Granada). The wave flume is 23 m long, 0.65 m wide and 1 m deep (1). Waves are generating by means of a pyston-type wave-maker placed at one end, equipped with an active wave absorption system. In the middle of the flume was positioned a sediment bed and a pebbles breakwater. The sediments were well-sorted with d_{50} = 0.32 mm, a relative density s = 2.65 and an repose angle of 31°. The breakwater was made of pebbles of mean diameter equal to 4 cm retained by a wire casing, and was buried in the sand for a depth of 5 cm.

The free surface elevation was measured with eight acoustic level sensors placed above the flume with a sample of frequency of 20Hz. Horizontal and vertical velocity measurements were recorded by a laser doppler velocimeter (LDV) with a minimum data rate of ≈ 30 Hz. The bottom profiles were recorded by a digital camera installed on a tripod, in normal plane 2m-away from the glass wall of flume. The camera took snapshots every 20 minutes.

Setup

Three bed and reflecting configurations were adopted. Table 1 lists the main parameters of the experiments carried out. More details of the experimental setup can be found in Cobos et al. (2016).

1. *RFP* A flat bed 2.5 m-long and 20 cm-deep with mid-reflecting conditions.

2. *RSP* A sloping bed 4 m-long a 1/20 steepness with mid-reflecting conditions.

3. *RFP* A sloping bed 4 m-long a 1/20 steepness. An impermeable wooden sheet of 3 cm-wide was

Test	Case	T (s)	H (cm)	L (cm)	u_{b0} (cm/s)	Ro	ψ	K	*Duration* (min)
001[a]	RFP	1.05	4	129					20
002[a]	RFP	1.05	5						20
003	RFP	1.05	6		23.8	10	11	0.504	160
004[a]	RFP	1.30	4	167					40
005	RFP	1.30	5		23.0	10	10	0.544	200
006[b]	RFP	1.30	6		28.2	9	15	0.503	200
007[a]	RSP	1.30	4						100
008[b]	RSP	1.30	5		22.8	10	10	0.550	1170
009[b]	RSP	1.70	4	227					40
010[b]	RSP	1.70	5		24.8	11	12	0.564	888
011[b]	RSF	1.30	5		28.0	9	15	0.908	894
012[b]	RSF	1.70	5		28.4	10	15	0.787	866

Table 1: Parameters of the experiments. Case column: 'R' stands for regular waves; 'I' for random (irregular) waves; 'S' for sloping bed; 'P' for partial reflection; and 'F' for full reflection. T is the period for regular waves; H their wave height; L is the corresponding wavelength; u_{b0} is the amplitude of the bottom velocity computed according to the potential flow theory, including the reflected component; $Ro = w_s/(\kappa u^*)$ is the Rouse number where w_s is the sediment settling velocity; and u^* is the friction velocity, $\kappa = 0.4$ is the von Kármán constant; $\psi = u_{b0}^2/((s-1)gd_{50})$ is the mobility number; and K stands for the modulus of the reflection coefficient. In the first column, the symbol [a] indicates that no sediment motion was recorded; [b] indicates that LDV velocity measurements are available.

located in front of the wall.

The modulus of reflection parameter K was obtained applying the method described in Baquerizo (1995) and Baquerizo et al. (1997).

Experimental procedure

During tests the acoustic level sensors record the free surface and a camera takes photos of the bed at regular interval times. Then LDV measures the velocity next to the bed along the flume. The bottom was flattened before starting a new test.

Image and bed analysis

The bottom profile was analyzed with image analysis [Baglio et al. (1998) and Faraci and Foti (2002)]. Briefly, the time series of snapshots were converted into a grey scale and then grouped into two sets by means of a k-means algorithm. The contour is emphasized using a Gabor filter, then a tracking algorithm locates the bed profile and, finally, each pixel is converted into the lab coordinates (Cobos et al., 2016).

After applying the image analysis technique to the experimental results, the resolution obtained ($\sim 0.6mm/px$) was found adequate to analyze the bed evolution in the spectral domain (Doucette and O'Donoghue, 2006). First, a band-passing frequency filter (FFT) was employed to the raw data in order to remove the noise. This technique was applied with a good estimation bounding the filter with 2nd and 98th percentile of the elevation distribution (Traykovski, 2007). The output data was splitted into ripple and sandbar profiles. Ripple profiles were obtained applying a high-pass filter with a cut frequency defined by visual inspection of the minimum variance between sandbars and ripples (Table 2). In order to homogenize the analysis we unified the cut frequency to $f_c = 0.005$ (1/mm).

The ripple and sandbar bed is developed by well-defined sections of the same length. Sandbars length is related to the wavelength as described in Carter et al. (1973). Sandbars appear every $L/2$ (Figure 2). Ripples developed in sandbars region while flats are observed in between (Gíslason et al., 2009). To remove the incidence of new growing ripples from another sandbar in the analysis, we chose sections $\sim L/2$ that bound one sandbar. Table 2 shows the edges of sandbars assuming that almost each sandbar domain behaves like a Control Volume with negligible sediment flux at their contours. The number of ripples included in every window is about 14. x_a and x_b define the start and end of the window. In some experiments, scour appears in the near breakwater region. For this reason, x_a is not placed at $x = 0$.

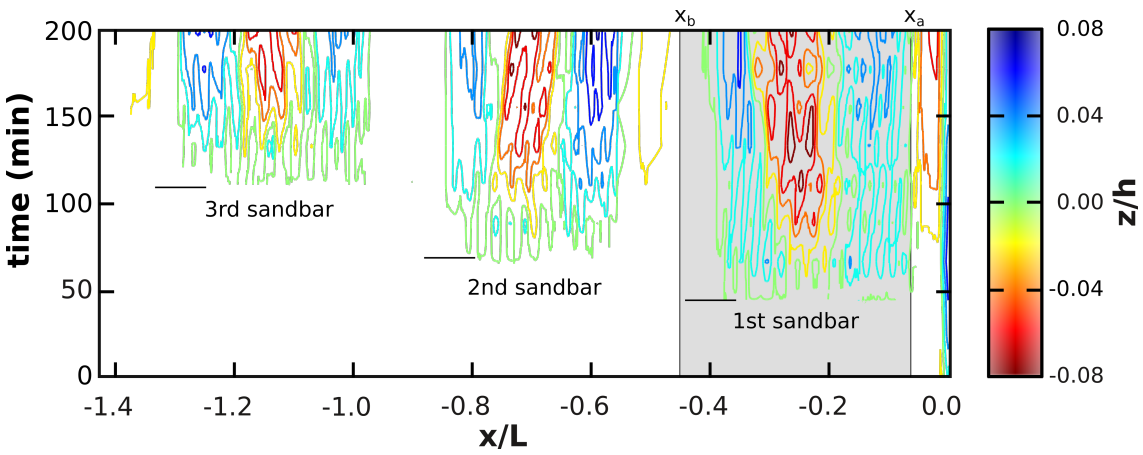

Figure 2: Description of the general process of ripple and sandbar development (test no.005). x_a **and** x_b **stand for the begining and the end of the window section.**

Test	$f_{c,min}$ (1/mm)	x_a (cm)	x_b (cm)
003	0.08867	0	60
005	0.09425	8	82
006	0.05498	7	87
008	0.08548	10	80
010	0.09664	25	105
011	0.08228	10	75
012	0.06916	22	107

Table 2: Certain parameter related to PSD-window. x_a **and** x_b **stand for the edge locations of the window.**

The spectral density analysis were conducted to every of the ripple bed profiles as described in Davis et al. (2004) or Smith and Sleath (2005). We applied the power-spectral-density (PSD) function to the bed sections. PSD was characterized by bed data of ~80 cm long (with more than 1536 points each transect) divided into 3 sections where the band width is about 512 points and without overlapping. Three different windows were tested without significant changes (Smith and Sleath, 2005).

RESULTS

In the experiments we found 2D orbital ripples (Wiberg and Harris, 1994) developing over sandbars. Regarding Table 1, Rouse and mobility numbers indicate that bedforms evolved under low energy conditions and bedload sediment transport regime. The ripples started to develop in a general motion as described by Losada and Desiré (1985).

Figure 3.a shows the PSD for test no.005 at the beginning of ripple growth ($1/3Duration$), in the middle of experiments duration ($2/3Duration$), and at the end ($Duration$). Data from Davis et al. (2004) in similar conditions for progressive waves are also shown for comparison purposes. At the beginning, similar spectra can be found in progressive and reflecting conditions. The ripples spatial frequencies are confined in a smaller frequency band than in the progressive test. PSD of frequency peaks show similar values (~500 mm^3) However, just 60 minutes later, sandbar starts to growth and strongly modify the PSD. The power spectral density peak is shifted to low frequencies that correspond to the largest ripples that appear in the tests. At the end of Davis et al. (2004) experiment, frequency peak is placed near $f_p = 0.015$ 1/mm and PSD up to 1100 mm^3. Depth differences between sandbar crest and troughs origin a new peak at low frequencies. This fact agrees with Traykovski (2007) suggestion that ripples growth in bimodal pattern in the field. Figure 3.a depicts two peaks at frequencies $f_1 = 0.0085$ 1/mm and $f_2 = 0.017$ 1/mm and PSD for both peaks of 400 mm^3 and 720 mm^3. From those ripples, the largest appear at the crest of sandbar.

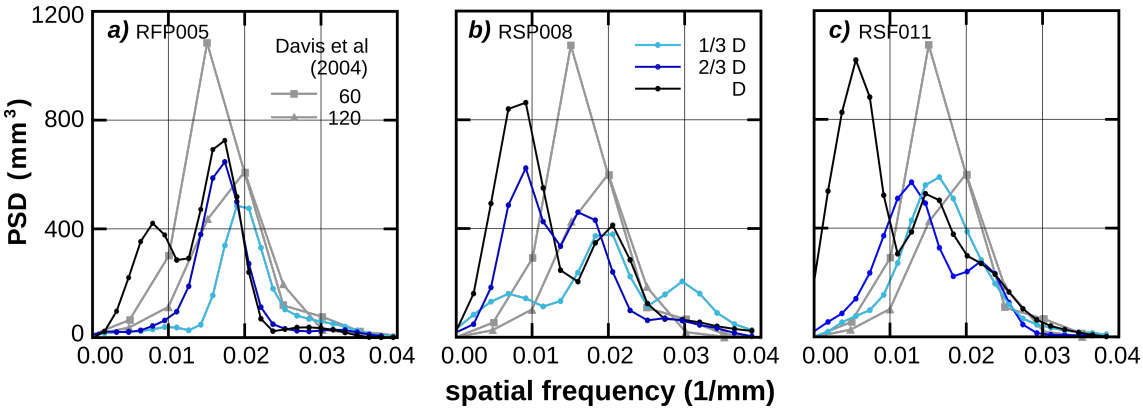

Figure 3: Power spectral density of ripple horizontal bed and sloping bottom under regular waves and mid- and high-reflecting conditions.

Figure 3.b shows the spectral analysis for test no.008. Again, data from Davis et al. (2004) are shown for comparison. At initial stages, ripple development is slower than for horizontal beds (Figure 3). However, the frequency band is largest than for previous experiments. Ripples of several lengths grow up. At the middle of test, the bimodal shape of the spectra is observed. Two peaks quite near appear with a PSD that overcomes the 400 mm^3. It is noticeable that the frequency peak linked to ripples placed at the crest of sandbar (~600 mm^3) is bigger than the peak linked to sandbar trough (~450 mm^3). Finally, at the end of experiments, the frequency distance between the two peaks increase. The low-frequency peak did not shift f_1 = 0.0095 1/mm, however, the high-frequency peak shifts to f_2 = 0.021 1/mm. As we can observed, the differences in frequencies between horizontal and sloping beds are important.

Figure 3.c shows the spectral analysis for test no.011. Data from Davis et al. (2004) are also drawn for comparison. In these experiments, the high-reflecting conditions rapidly modify the bed profile. At the beginning, a deep scour appear near at the toe of the breakwater. Ripples develop faster than in previous experiments. A normal distribution of the frequency is now clearly observed (Traykovski, 2007). The next steps is similar to previous experiments with the difference that at equilibrium stage, a similar PSD-value of the low-frequency peak as Davis et al. (2004) is found (~ 1100mm^3). Frequency peaks are now found in smaller frequencies than before (f_1 = 0.006 1/mm and f_2 = 0.014 1/mm). We can observed that tests 008 and 011 reach an equilibrium stage, if it exists under regular waves, in front of reflective conditions (Cobos et al., 2016), however, it is quite probable that test no.005 did not reach.

Ripple height

A characteristic ripple height of the bed profile in a sandbar window η_r was obtained from PSD of our experiments. Following Davis et al. (2004),

$$\eta_r = 2.8\sqrt{\int_{f_{s1}}^{f_{s2}} S_r df} \tag{1}$$

where S_r is the ripple variance spectrum (mm^3), f_s is the spatial frequency (1/mm) and f_{s1}, and f_{s2} are the upper and lower bounds defining the ripple spatial frequencies present in the spectrum. Due to the bimodal pattern found in the ripple bed geometry, we computed isolated the height of high and low frequency bands. Regarding Figure 3 where the final spectrum is shown, we employed two frequency bands [0 - f_l] and [f_l - 0.04] to consider the different growths of ripple on sandbar crests and troughs. These cut values were kept in the following analysis.

Figure 4 shows the ripple height of the *a* test no.005 (RFP); *b* test no.008 (RSP), and, *c* test no.011 (RSF). Flat bed can be observed till $1/3D$ under regular waves. Then, a quickly increase of ripple height appears. Two clear different growing mechanisms appear. The height of ripples constrained in the high-frequency band (solid lines) develops faster than those bounded by the low-frequency band (dashed lines). The growth mechanism at sandbar crest accelerates the increase of ripple geometry at the same time than sandbar growth (Figure 2). This is noticeable in Figures 4.a and .c, however, it is not so evident in Figure

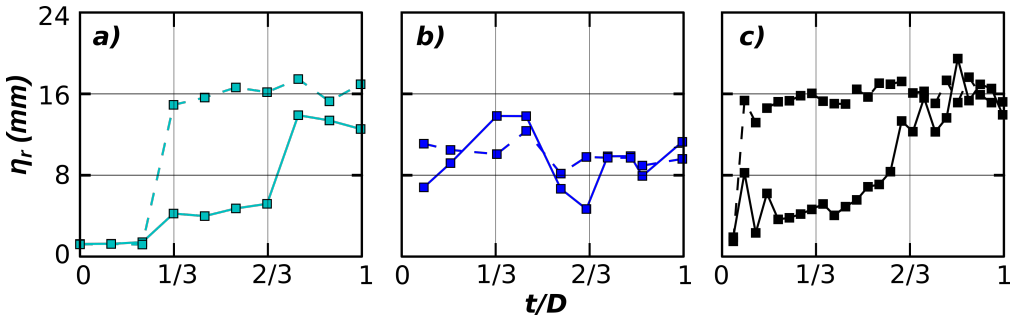

Figure 4: Characteristic ripple height along the experiment. *a*) Test no.005; *b*) Test no.008; and, *c*) Test no.011. Lines refer to the ripple develop of the low-frequency band (solid lines) and high-frequency band (dashed lines).

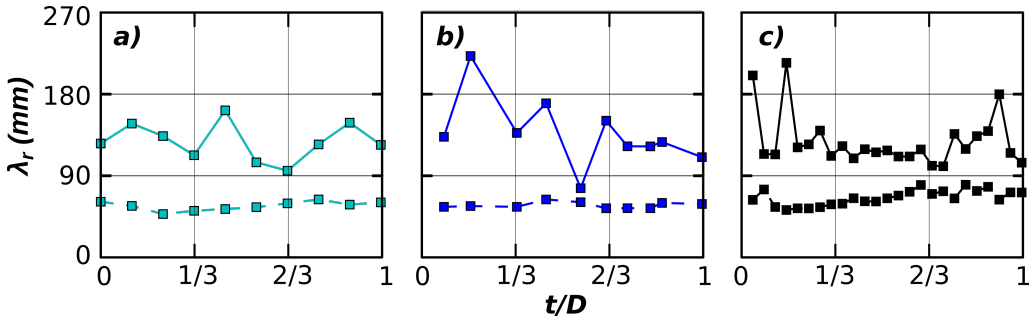

Figure 5: Characteristic ripple length along the experiment. *a*) Test no.005; *b*) Test no.008; and, *c*) Test no.011. Lines refer to the ripple develop of the low-frequency band (solid lines) and high-frequency band (dashed lines).

4.b. Our experiments show that at equilibrium the ripple height tends to the same value (16 mm) even for several reflecting conditions, but, with different time scales of evolution. Test no.008 (Figure 4.b) shows heights relatively smaller than another tests maybe due to the equilibrium was not reached.

Ripple length

The characteristic ripple length related to the sandbar window λ_r was obtained from PSD. Following Davis et al. (2004),

$$\lambda_r = \frac{\int_{f_{s1}}^{f_{s2}} S_r^4(f_s) df_s}{\int_{f_{s1}}^{f_{s2}} f_s S_r^4(f_s) df_s} \tag{2}$$

Figure 5 shows the temporal evolution of ripple length for several conditions. Our results agree with previous studies that described the ripple evolution at almost stationary stage (see for example Wiberg and Harris (1994)). As previously noted, sandbars create two well-defined ripple patterns. The longest ripple lengths appear at the crest of sandbars ($\lambda_r = 120mm$) whilst the shortest ripple lengths appear in the troughs ($\lambda_r = 75mm$).

Ripple steepness

The characteristic ripple steepness was computed as the quotient of η_r by $/lambda_r$. Figure 6 shows the ripple steepness under several conditions. As previously noted, ripple length plays a key role in the steepness. As before, two well-defined steepness were observed from our experiments. Surprisingly, steeper ripples can be found at the high-frequency band that decrease gradually untill reaching the equilibrium. On the other hand, ripple steepness of low-frequency band increases slowly.

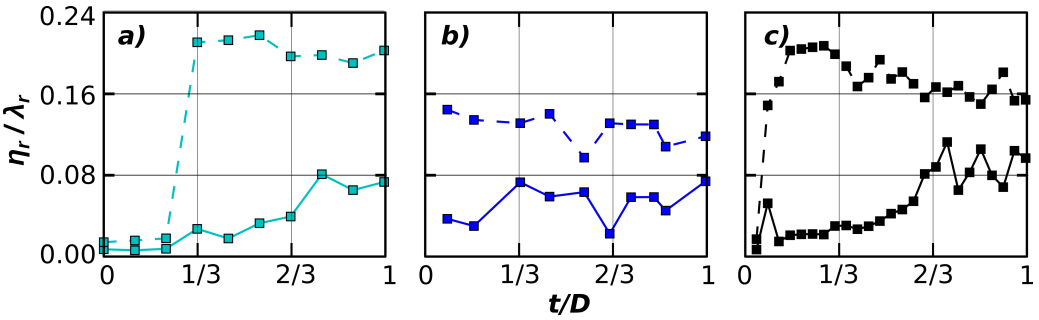

Figure 6: Characteristic ripple steepness along the experiment. *a*) Test no.005; *b*) Test no.008; and, *c*) Test no.011. Lines refer to the ripple develop of the low-frequency band (solid lines) and high-frequency band (dashed lines).

DISCUSSION AND CONCLUSION

This study presents the experimental research on bedforms under the wave forcing for low energy conditions (bedload sediment transport regime and waves that do not break) for horizontal and sloping beds, and mid- and high-reflecting conditions. A spatial modulation on ripple geometry as described in Landry (2011) was observed. This modulation cames from the spatial pattern created by the incident and reflected waves that forced the generation of the sandbars that finally modified the ripple geometry. While ripple height converged at equilibrium at the crests and troughs of sandbars, ripple length (and steepness) did not. Two space-time scales where observed in our experiments that were related to faster/lower processes in the troughs/crests.

Ripples in mid- and high-reflecting conditions are affected by the spatial pattern that create the superposition of the incoming and reflected waves. Our experiments showed that the incidence of reflection that overcame the threshold defined in Carter et al. (1973) created sandbars. These sandbars modified the evolution patterns which were produced in the sandbar crests and troughs (Cobos et al., 2016). The two families found in the analysis were separated by a cut frequency defined by the minimum PSD at the end of tests. It seems that ripple migration depends on the stage of development of the first bar (close to the reflective structure).

Our experiments depicted that at initial stages, the rolling grain mechanism built up enough disturbances and it starts to disrupt the bottom boundary layer as described Bagnold and Taylor (1946). Then, ripples followed two growth mechanisms: (i) ripples in the low-frequency band are lengthening as their height in a increasing process called "the variance cascade" (Jain and Kennedy, 1974); (ii) ripples in the high-frequency band are smoothly shortening while their height keep almost constant. However, although the development of different ripple bands converges till the same height, the same finding does not apply to ripple length, and therefore, not to the ripple steepness.

Similar ripple height in flat bed with mid reflection and sloping bed with full reflection were observed whilst smaller ripples heights were found in the mid-reflecting conditions for sloping beds. Ripple lengths were found nearly constant for all conditions. The lack of longer tests in certain experiments beside to the limited number of ripples in each window may not adequately reproduce the ripple geometry. Furthermore, more experiments should be carried out with several grain diameters, reflecting, and wave conditions (also random waves).

Differences in the time evolution of ripples characteristics were highlighted in our experiments, however almost similar 'equilibrium' geometry was detected in all tests. This fact agree which observed Messaros and Bruno (2011) with regular waves under flat and sloping beds.

ACKNOWLEDGMENTS

This research was partially funded by the Campus Excelencia Internacional del Mar (Cei-MAR) and a Microproject ST1-2015 titled *Formación y evolución de formas de lecho en la zona de asomeramiento de playas reflejantes* from CEI-Biotic Granada.

References

J. R. Allen. *Sedimentary Structures Their Character and Physical Basis Volume I*, volume 30, Part A of *Developments in Sedimentology*. Elsevier, 1982.

A. Ávila, A. Baquerizo, and M. A. Losada. Edge wave scattering by coastal structures on arbitrary bathymetry. *Journal of Coastal Research*, pages 1536–1544, 2008.

S. Baglio, C. Faraci, and E. Foti. Structured light approach for measuring sea ripple characteristics. In *OCEANS '98 Conference Proceedings*, volume 1, pages 449–453 vol.1, Sep 1998. doi: 10.1109/OCEANS.1998.725787.

R. A. Bagnold and G. Taylor. Motion of waves in shallow water. interaction between waves and sand bottoms. *Proceedings of the Royal Society of London A: Mathematical, Physical and Engineering Sciences*, 187(1008):1–18, 1946. doi: 10.1098/rspa.1946.0062.

A. Baquerizo. *Wave Reflection on Beaches: Methods of Assessment and. Forecasting*. PhD thesis, Ph.D. Thesis, University of Cantabria (in Spanish), 1995.

A. Baquerizo, M. Losada, J. Smith, and N. Kobayashi. Cross-shore variation of wave reflection from beaches. *Journal of Waterway, Port, Coastal, and Ocean Engineering*, 123(5):274–279, 1997. doi: 10.1061/(ASCE)0733-950X(1997)123:5(274).

A. Baquerizo, M. Losada, and I. Losada. Edge wave scattering by a coastal structure. *Fluid Dynamics Research*, 31(4):275–287, 2002.

A. Baquerizo, M. Ortega-SÁnchez, and M. A. Losada. Mass transport and related bedforms induced by phase-locked edgewaves in a groin. In *Coastal Engineering 2004: (In 4 Volumes)*, pages 2694–2702. World Scientific, 2005.

M. I. Benedicto, M. Losada, and I. Sánchez-Arévalo. Dependence of the stability of mound breakwaters on the reflection process. In *Coastal Structures 2003*, pages 91–99. 2004.

T. G. Carter, P. L. Liu, and C. C. Mei. Mass-transport by waves and offshore sand bedforms. *Journal of the Waterways Harbors and Coastal Engineering Division-ASCE*, 99(WW2):165–184, 1973.

M. Cobos, C. L., L. S., B. A., and L. M.A. Ripple and sandbar dynamics under mid-reflecting conditions with a porous vertical breakwater. *Submitted to Coastal Engineering*, 2016.

J. P. Davis, D. J. Walker, M. Townsend, and I. R. Young. Wave-formed sediment ripples: Transient analysis of ripple spectral development. *Journal of Geophysical Research: Oceans*, 109(C7), 2004. ISSN 2156-2202. doi: 10.1029/2004JC002307. C07020.

J. R. Dingler. *Wave formed ripples in nearshore sands*. Ph.D. thesis, University of California, San Diego, 1974.

J. S. Doucette and T. O'Donoghue. Response of sand ripples to change in oscillatory flow. *Sedimentology*, 53(3):581–596, 2006. ISSN 1365-3091. doi: 10.1111/j.1365-3091.2006.00774.x.

C. Faraci and E. Foti. Geometry, migration and evolution of small-scale bedforms generated by regular and irregular waves. *Coastal Engineering*, 47(1):35 – 52, 2002. ISSN 0378-3839. doi: 10.1016/S0378-3839(02)00097-2.

K. Gíslason, J. Fredsøe, R. Deigaard, and B. M. Sumer. Flow under standing waves: Part 1. shear stress distribution, energy flux and steady streaming. *Coastal Engineering*, 56(3):341 – 362, 2009. ISSN 0378-3839. doi: 10.1016/j.coastaleng.2008.11.001.

D. L. Inman. *Wave-generated ripples in nearshore sands*. Beach Erosion Board, Tech. Memo 100. U. S. Army Corps of Engineers, 1957.

S. C. Jain and J. F. Kennedy. The spectral evolution of sedimentary bed forms. *Journal of Fluid Mechanics*, 63(02):301–314, 1974.

B. J. Landry. *Sand bed morphodynamics under water waves and vegetated conditions*. PhD thesis, University of Illinois at Urbana-Champaign, 2011.

M. A. Losada and J. M. Desiré. Incipient motion on a horizontal granular bed in non-breaking water waves. *Coastal Engineering*, 9(4):357 – 370, 1985. ISSN 0378-3839. doi: 10.1016/0378-3839(85)90017-1.

M. Manohar. *Mechanics of bottom sediment movement due to wave action*. Dayton : Armed Services Technical Information Agency, 1955.

R. C. Messaros and M. S. Bruno. Laboratory investigation of bedform geometry under regular and irregular surface gravity waves. *Journal of Coastal Research*, pages 94–103, 2011. doi: 10.2112/JCOASTRES-D-09-00062.1.

G. Mogridge and J. Kamphuis. Experiments on bed form generation by wave action. *Proceedings Coastal Engineering 1972*, pages 1123–1142, 1972. doi: 10.1061/9780872620490.063.

P. Nielsen. Dynamics and geometry of wave-generated ripples. *Journal of Geophysical Research: Oceans*, 86(C7):6467–6472, 1981. ISSN 2156-2202. doi: 10.1029/JC086iC07p06467.

P. Nielsen. *Coastal Bottom Boundary Layers and Sediment Transport*. Advanced series on ocean Engineering. World Scientific, 1992. ISBN 9789810204730.

E. Sánchez-Badorrey, M. Losada, and J. Rodero. Sediment transport patterns in front of reflective structures under wind wave-dominated conditions. *Coastal Engineering*, 55(7):685–700, 2008.

D. Smith and J. F. Sleath. Transient ripples in oscillatory flows. *Continental Shelf Research*, 25(4):485 – 501, 2005. ISSN 0278-4343. doi: 10.1016/j.csr.2004.10.012.

P. Traykovski. Observations of wave orbital scale ripples and a nonequilibrium time-dependent model. *Journal of Geophysical Research: Oceans*, 112(C6), 2007. ISSN 2156-2202. doi: 10.1029/2006JC003811. C06026.

P. L. Wiberg and C. K. Harris. Ripple geometry in wave-dominated environments. *Journal of Geophysical Research: Oceans*, 99(C1):775–789, 1994. ISSN 2156-2202. doi: 10.1029/93JC02726.